Cahn-Hoffman capillarity vector thermodynamics for liquid crystal interfaces

Ae-Gyeong Cheong and Alejandro D. Rey*
Department of Chemical Engineering, McGill University, 3610 University Street, Montreal, Quebec, Canada H3A 2B2
(Received 25 March 2002; published 9 August 2002)

The classical Cahn-Hoffman capillarity vector formalism for anisotropic interfaces, widely used to analyze capillary and surface patterning processes in metallurgical systems, is applied to nematic liquid crystalline interfaces. The nematic capillarity vector is derived and expressed in terms of nematic surface energies. Expressions for surface tension forces on surface line elements are derived and shown to include the usual tangential forces as well as normal forces driven by surface tension anisotropy. The connections between interfacial rotational effects, surface tension anisotropy, and bending stresses are established. The vector formalism is shown to be a tractable and simple method to analyze capillarity processes in nematic liquid crystals. The application of the formalism to a straight nematic triple line shows that the interface configuration should be such that the projection of the sum of the three capillarity vectors on a plane normal to the contact line vanishes.

DOI: 10.1103/PhysRevE.66.021704 PACS number(s): 61.30.Dk, 61.30.Hn, 68.05.Cf

I. INTRODUCTION

The surface physics of nematic liquid crystals is currently an active area of research [1–6] since many applications of liquid crystalline materials involve multiphase systems, where interfaces play significant roles. Interfacial orientation phenomena and orientational transitions in well-defined geometries are well characterized experimentally [1–3] and theoretically [4–8]. On the other hand, deforming interphases and shape characterization are less characterized. This paper deals with capillarity models of interfacial forces that drive shape determination in anisotropic nematic liquid crystals (NLCs) materials. Examples of applications of the capillarity models include determination of contact angles, droplet shapes, and triple line phenomena. Although static and dynamical interfacial models for NLCs have been presented [4–14], there is a need to formulate simple and more tractable models. This paper presents a capillarity model based on the widely used Cahn-Hoffman formalism of capillarity for anisotropic surfaces [14]. Since the Cahn-Hoffman formalism was developed for anisotropic surfaces, it follows that the formalism is also applicable to anisotropic NLCs. The main objectives of this paper are (1) to adapt the widely used Cahn-Hoffman formalism to NLCs surfaces and interfaces, (2) to establish the correspondence between the nematic Cahn-Hoffman equations and the classical interfacial mechanics of NLCs presented in [12,13], and (3) to show the usefulness of the approach by analyzing the interface configuration at a straight triple line junction. The organization of this paper is as follows. Section II presents the main derivations and results of the Cahn-Hoffman equations, Sec. III presents the derivation of the nematic Cahn-Hoffman equations, Sec. IV presents the correspondence between the nematic Cahn-Hoffman equation and the surface stress tensor equation presented in [12,13], Sec. V presents an application of the Cahn-Hoffman equations to the nematic triple line junction, and Sec. VI presents the conclusions. In what follows we refer only to surfaces but the model applies equally to interfaces.

II. THE CAHN-HOFFMAN CAPILLARITY VECTOR FOR ANISOTROPIC SURFACES

This section summarizes the Cahn-Hoffman formalism as given in [14]. For anisotropic systems, the surface free energy density γ is a function of the surface unit normal $\mathbf{k}$: $\gamma(\mathbf{k})$. The capillarity vector $\boldsymbol{\xi}(\mathbf{k})$ is defined by the gradient of the scalar field $r\gamma$:

$$\boldsymbol{\xi}(\mathbf{k}) = \nabla(r\gamma), \tag{1a}$$

$$\mathbf{r} = r\mathbf{k}, \tag{1b}$$

where r is the magnitude of surface position vector $\mathbf{r}$. Noting the dependence $\boldsymbol{\xi}(\mathbf{k})$, the gradient of $r\gamma$ yields

$$d(r\gamma) = \nabla(\mathbf{r}\gamma)\cdot d\mathbf{r}, \tag{2a}$$

$$r d\gamma + \gamma dr = \boldsymbol{\xi}\cdot d(r\mathbf{k}) = r\boldsymbol{\xi}\cdot d\mathbf{k} + \boldsymbol{\xi}\cdot\mathbf{k} dr, \tag{2b}$$

and therefore

$$\boldsymbol{\xi}_{\perp} = \boldsymbol{\xi}\cdot\mathbf{k}\mathbf{k} = \gamma\mathbf{k}, \tag{3a}$$

$$d\gamma = \boldsymbol{\xi}\cdot d\mathbf{k}. \tag{3b}$$

Using Eq. (3b) it follows that

$$\boldsymbol{\xi}\cdot\frac{d\mathbf{k}}{d\theta} = \frac{d\gamma}{d\theta}, \tag{4}$$

where $|d\mathbf{k}| = d\theta$ is a small rotation angle. Since the unit tangent vector is given by $\mathbf{t} = d\mathbf{k}/d\theta$, it follows that $\boldsymbol{\xi}_{\parallel} = \boldsymbol{\xi}\cdot\mathbf{t} = d\gamma/d\theta$. The selected tangential component of the capillarity vector $\boldsymbol{\xi}$ is the one that maximizes the increase of surface energy with rotation, and hence

*FAX: (514) 398-6678. Email address: alejandro.rey@mcgill.ca

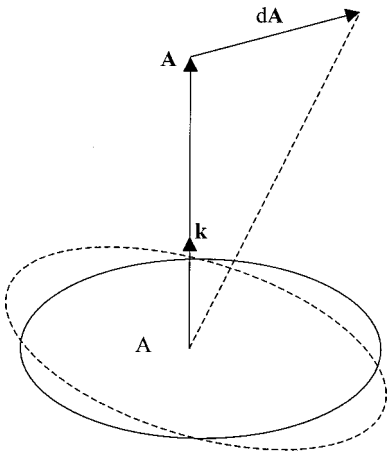

FIG. 1. Schematic of a surface patch indicating that the two modes of surface energy increase: (a) dilation, increase of surface area **A**; (b) rotation, tilt of area vector **A**. Adapted from [14].

$$\boldsymbol{\xi}_{\parallel} = \boldsymbol{\xi} \cdot \mathbf{I}_s = \left(\frac{d\gamma}{d\theta} \right)_{\max} \mathbf{t}_0 , \tag{5}$$

where $\mathbf{t}_0$ is the unit tangent vector along which $d\gamma/d\theta$ has the maximum rate of increase. For anisotropic surfaces there is a principal orthogonal coordinate frame $(\mathbf{t}_0, \mathbf{b}_0)$, and the rotation of the unit surface normal $\mathbf{k}$ around $\mathbf{b}_0$ produces the maximum increase in surface energy. The principal frame is selected by the main anisotropic axes of the surface. Anisotropic surfaces can change surface energy by dilation and by rotation. Figure 1 shows an element of area $A = \mathbf{A} \cdot \mathbf{k}$ and surface unit normal $\mathbf{k}$ that undergoes expansion and rotation. Since γ is a function of $\mathbf{k}$, the surface energy γ can be increased by expansion and by rotation of $\mathbf{k}$. Figure 2 shows the components of $\boldsymbol{\xi}$, their magnitudes, and the principal frame $(\mathbf{t}_0, \mathbf{b}_0)$. Figure 3 shows a schematic of the capillarity

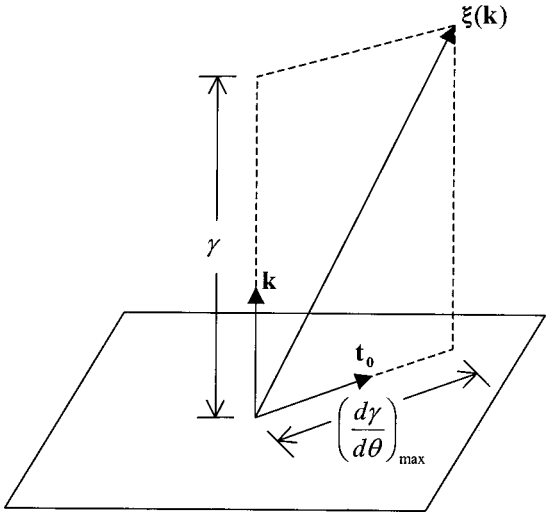

FIG. 2. Schematic of the capillarity vector $\boldsymbol{\xi}$, its normal $\boldsymbol{\xi}_{\perp}$, and tangential components $\boldsymbol{\xi}_{\parallel}$, and principal surface coordinate frame $(\mathbf{t}_0, \mathbf{b}_0)$. Adapted from [14].

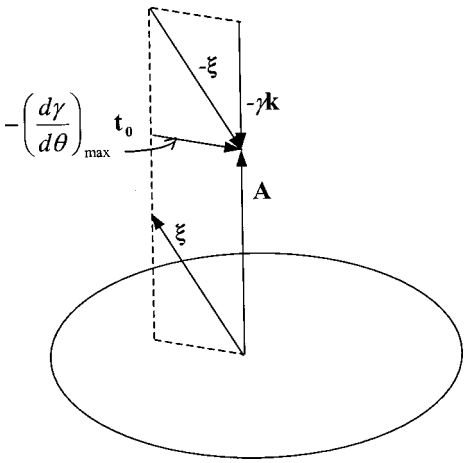

FIG. 3. Schematic of the effect of the capillarity vector $-\boldsymbol{\xi}$ and its components on the surface area vector **A**. The normal component tends to shrink the area, while the tangential components tends to rotate the area vector to reduce surface energy. Adapted from [14].

vectors $\boldsymbol{\xi}$ and $-\boldsymbol{\xi}$, and the normal $-\boldsymbol{\xi}_{\perp}$ and tangential $-\boldsymbol{\xi}_{\parallel}$ components of $-\boldsymbol{\xi}$. The vector $-\boldsymbol{\xi}$ represents the surface force acting on the area vector $\mathbf{A}$ tending to shrink $(-\boldsymbol{\xi}_{\perp})$ and rotate $(-\boldsymbol{\xi}_{\parallel})$ the surface. For isotropic surface $\boldsymbol{\xi}_{\parallel} = 0$ and no rotational effects appear.

The capillarity vector $\boldsymbol{\xi}$ is needed to compute the surface tension force density $\boldsymbol{\sigma}$. The surface tension force per unit length σ acting on a line element oriented along a unit tangent vector $\mathbf{l}$ is $\boldsymbol{\sigma} = \boldsymbol{\xi} \times \mathbf{l}$, from which the following tangential and normal components are obtained:

$$\boldsymbol{\sigma}_{\parallel} = \boldsymbol{\xi}_{\perp} \times \mathbf{l} = \gamma(\mathbf{k} \times \mathbf{l}) = \gamma \boldsymbol{\nu}, \tag{6a}$$

$$\boldsymbol{\nu} = \mathbf{k} \times \mathbf{l}, \tag{6b}$$

$$\boldsymbol{\sigma}_{\perp} = \boldsymbol{\xi}_{\parallel} \times \mathbf{l} = \left(\frac{d\gamma}{d\theta} \right)_{\max} (\mathbf{t}_0 \times \mathbf{l}). \tag{7}$$

Since $\boldsymbol{\nu} = \mathbf{k} \times \mathbf{l}$ for any $\mathbf{l}$, the magnitude of the tangential surface force $\sigma_{\parallel}$ is always γ. On the other hand, the normal surface force $\boldsymbol{\sigma}_{\perp}$ depends on the vector $\mathbf{t}_0 \times \mathbf{l}$. Thus $\boldsymbol{\sigma}_{\perp} = \mathbf{0}$ for $\mathbf{t}_0 \| \mathbf{l}$ and $\boldsymbol{\sigma}_{\perp} = (\boldsymbol{\sigma}_{\perp})_{\max}$ for $\mathbf{t}_0 \perp \mathbf{l}$.

III. THE CAHN-HOFFMAN CAPILLARITY VECTOR FOR NEMATIC SURFACES

For a NLC surface the nematic ordering is defined by the three-component orientation vector known as the director, $\mathbf{n} = \mathbf{n}(\mathbf{r})$, where $\mathbf{n} \cdot \mathbf{n} = 1$, $\mathbf{r} = r\mathbf{k}$ is the surface position vector, and $\mathbf{k}$ is the surface unit normal, as before. A useful decomposition of the surface director field into tangential and normal components is $\mathbf{n}_{\parallel} = \mathbf{I}_s \cdot \mathbf{n}$ and $\mathbf{n}_{\perp} = \mathbf{k}\mathbf{k} \cdot \mathbf{n}$, where $\mathbf{I}_s = \mathbf{I} - \mathbf{k}\mathbf{k}$ is the 2×2 unit surface dyadic, and $\mathbf{I}$ is the 3×3 volumetric unit tensor. To develop the Cahn-Hoffman capillarity vector for nematic surfaces we use the well-known Rapini-Papoular surface free energy density γ given by [15]

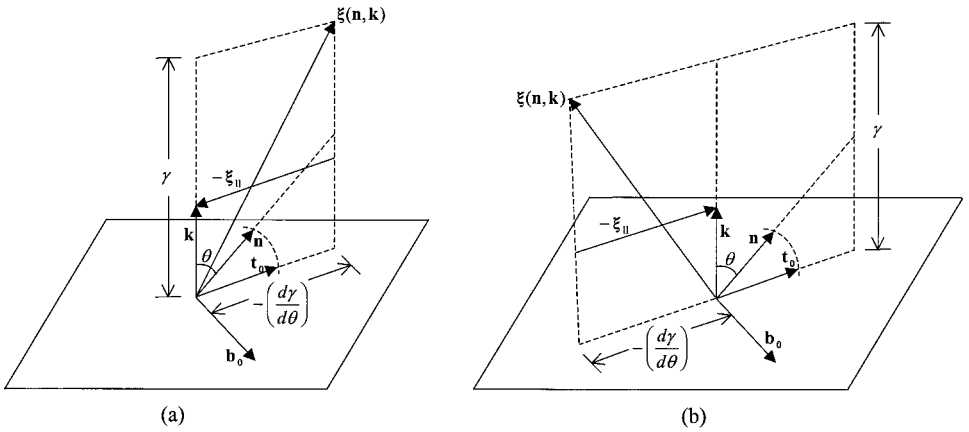

FIG. 4. Schematic of the main vectors in the nematic Cahn-Hoffman vector thermodynamics for (a) planar easy axis ($-d\gamma/d\theta>0$) and (b) homeotropic easy axis ($-d\gamma/d\theta<0$). The principal surface frame $(\mathbf{t}_0,\mathbf{b}_0)$ is selected by the director orientation.

$$\gamma(\mathbf{n}\cdot\mathbf{k},T)=\gamma_0(T)+\gamma_{\mathrm{an}}(\mathbf{n}\cdot\mathbf{k},T),$$
$$\gamma_{\mathrm{an}}(n\cdot k,T)=\frac{\gamma_2}{2}(T)\ \ [\mathbf{n}\cdot\mathbf{k}]^2, \tag{8}$$

where γ_0 is the isotropic contribution and γ_{an} is the anisotropic, anchoring energy, contribution. Higher order expansions are easily incorporated into Eq. (8), but the present expression suffices for the scope of this paper. To find the nematic capillarity vector $\boldsymbol{\xi}$ we use definition (1):

$$\boldsymbol{\xi}(\mathbf{n},\mathbf{k})=\boldsymbol{\nabla}[r\,\gamma(\mathbf{k})], \tag{9a}$$

$$\mathbf{r}=r\mathbf{k}, \tag{9b}$$

where the director $\mathbf{n}$ in the surface energy is kept constant: $\gamma(\mathbf{k})$. Computing the gradient of $r\gamma$ using $r=r(\mathbf{r},\mathbf{k})$ and $\mathbf{k}=\mathbf{k}(\mathbf{r})$ gives

$$\boldsymbol{\xi}(\mathbf{n},\mathbf{k})=\boldsymbol{\nabla}[r\,\gamma(\mathbf{k})]=\gamma\frac{\partial r}{\partial\mathbf{r}}+r\frac{d\gamma}{d\mathbf{r}}=\gamma\mathbf{k}+\mathbf{I}_s\cdot\frac{d\gamma}{d\mathbf{k}}, \tag{10}$$

where the following results have been used:

$$\frac{\partial r}{\partial\mathbf{r}}=\mathbf{k}, \tag{11a}$$

$$\frac{d\gamma}{d\mathbf{r}}=\mathbf{I}_s\cdot\frac{d\gamma}{d\mathbf{k}}\cdot\frac{\partial\mathbf{k}}{\partial\mathbf{r}}=\mathbf{I}_s\cdot\frac{d\gamma}{d\mathbf{k}}\left(\frac{1}{r}\right). \tag{11b}$$

Thus the components of the capillarity vector for nematic surfaces and interfaces are

$$\boldsymbol{\xi}_\perp=\gamma\mathbf{k},\quad \boldsymbol{\xi}_\parallel=\mathbf{I}_s\cdot\frac{d\gamma}{d\mathbf{k}}=(\mathbf{I}_s\cdot\mathbf{n})\frac{d\gamma}{d(\mathbf{n}\cdot\mathbf{k})}=\gamma'\mathbf{n}_\parallel, \tag{12}$$

where $\gamma'=d\gamma/d(\mathbf{n}\cdot\mathbf{k})$. To put $\boldsymbol{\xi}_\parallel$ in the Cahn-Hoffman form we let θ be the angle between the unit normal $\mathbf{k}$ and the director $\mathbf{n}$, and get

$$\xi_\parallel=\mathbf{I}_s\cdot\frac{d\gamma}{d\mathbf{k}}=\left(\frac{d\gamma}{d\theta}\right)_{\max}\mathbf{t}_0, \tag{13a}$$

$$\left(\frac{d\gamma}{d\theta}\right)_{\max}=\left(-\frac{d\gamma}{d\theta}\right), \tag{13b}$$

$$\mathbf{t}_0=\frac{\mathbf{n}_\parallel}{|\mathbf{n}_\parallel|}. \tag{13c}$$

Thus the maximum rate of increase of γ is just $-d\gamma/d\theta$, and the selected tangential vector $\mathbf{t}_0$ is the tangential unit vector along the surface projection of the director: $\mathbf{n}_\parallel$. In nematic surfaces the principal frame $(\mathbf{t}_0,\mathbf{b}_0)$ is defined by the intersection of the **k**-**n** plane and the surface. Thus nematic surfaces may decrease the surface energy by contraction or by rotation of the unit normal around an axis that is perpendicular to the surface projection of the director. The nematic surface behavior is isotropic only if

$$\boldsymbol{\xi}_\parallel=\mathbf{n}_\parallel\frac{d\gamma}{d(\mathbf{n}\cdot\mathbf{k})}=\mathbf{0}, \tag{14}$$

which is possible when $\mathbf{n}_\parallel=\mathbf{0}$ or when $d\gamma/[d(\mathbf{n}\cdot\mathbf{k})]=0$. When $\mathbf{n}$ is parallel to $\mathbf{k}$, the surface is isotropic. The directors $\mathbf{n}^*$ corresponding to the stable extrema of γ are known as the easy axes and are (i) planar, $\gamma_2>0$, $n_\parallel^*=1$; and (ii) homeotropic, $\gamma_2<0$. Figure 4(a) shows $\mathbf{k}$, $\mathbf{n}$, $\mathbf{t}_0$, $\mathbf{b}_0$, ξ, $-\xi_\parallel$ vectors for a planar easy axis. Rotation of $\mathbf{k}$ around $\mathbf{b}_0$ in the direction imposed by $-\xi_\parallel$ gives the fastest rate of decrease in anchoring energy; in this case $-d\gamma/d\theta>0$. Figure 4(b) shows $\mathbf{k}$, $\mathbf{n}$, $\mathbf{t}_0$, $\mathbf{b}_0$, ξ, $-\xi_\parallel$ vectors for a homeotropic easy axis. Rotation of $\mathbf{k}$ around $\mathbf{b}_0$ in the direction imposed by $-\xi_\parallel$ gives the fastest rate of decrease in anchoring energy; in this case $-d\gamma/d\theta<0$.

For a nematic surface the components of the surface tension force per unit length, σ, acting on a line element oriented along a unit tangent vector $\mathbf{l}$ are

$$\boldsymbol{\sigma}_\parallel=\boldsymbol{\xi}_\perp\times\mathbf{l}=\gamma(\mathbf{k}\times\mathbf{l})=\gamma\boldsymbol{\nu}, \tag{15}$$

$$\boldsymbol{\sigma}_\perp=\boldsymbol{\xi}_\parallel\times\mathbf{l}=\frac{d\gamma}{d(\mathbf{n}\cdot\mathbf{k})}\mathbf{n}_\parallel\times\mathbf{l}. \tag{16}$$

Thus the normal surface tension force per unit length acting on a line oriented along $\mathbf{l}$ is zero only if $\boldsymbol{\xi}_\parallel=\mathbf{0}$ or if $\mathbf{n}_\parallel\|\mathbf{l}$. Barring these possibilities, a line on a nematic surface is

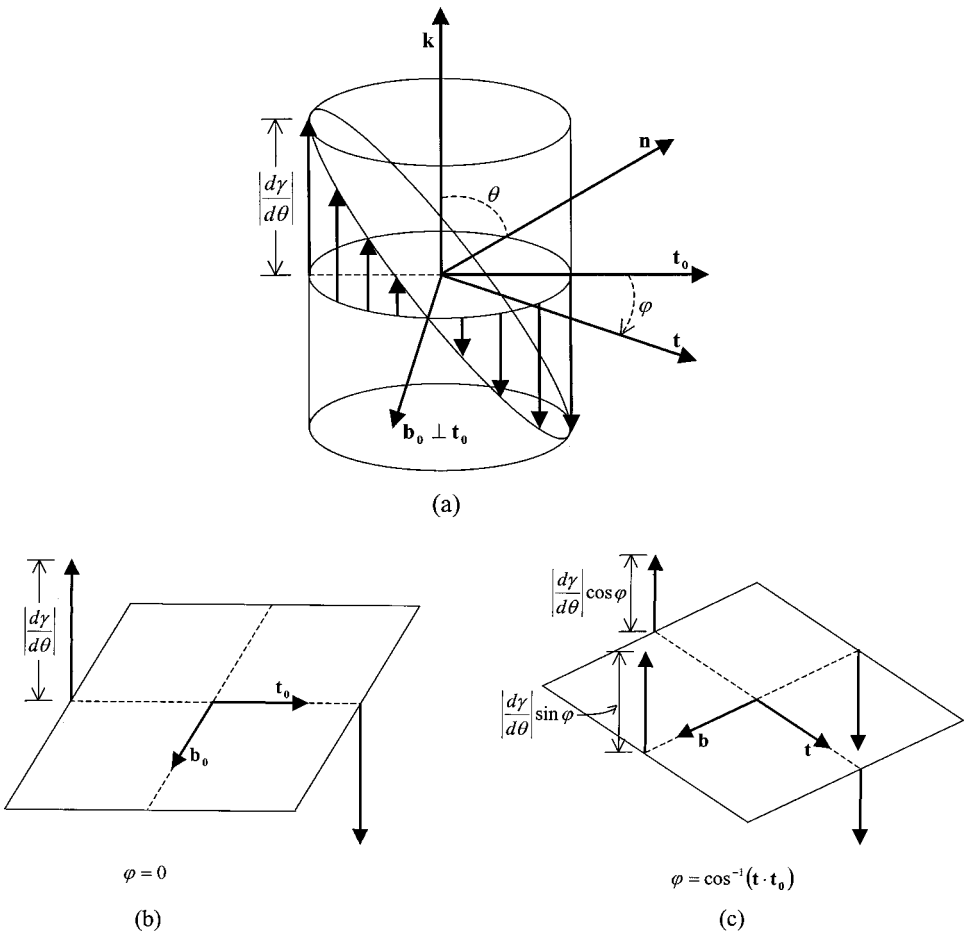

FIG. 5. (a) Schematic of the bending stress cylinder $\mathbf{T}^b$ in relation to the main surface vectors and main frame $(\mathbf{t}_0,\mathbf{b}_0)$. (b) Schematic of the single principal bending stress on a surface element oriented along the principal frame $(\mathbf{t}_0,\mathbf{b}_0)$. (c) Schematic of the two bending stresses on a surface element oriented along a nonprincipal frame $(\mathbf{t},\mathbf{b})$.

subjected to a normal force, unlike isotropic surfaces. This normal force plays a role in the balance of forces at contact lines and triple lines, where if one of the intersecting surfaces is nematic, the classical Neumann tangential capillary vector equation must be augmented to include the normal vector force $\boldsymbol{\sigma}_\perp$ [12].

IV. CORRESPONDENCE OF THE CAHN-HOFFMAN CAPILLARITY VECTOR AND THE ELASTIC SURFACE STRESS TENSOR

The previous model of interfacial nematostatics [12,13] is based on the elastic surface stress tensor $\mathbf{T}$. This fundamental quantity defines the capillary pressure p_c, $p_c=-(\nabla\cdot\mathbf{T})\cdot\mathbf{k}$, and the surface tension force $\boldsymbol{\sigma}$ on a surface line along $\mathbf{l}$: $\boldsymbol{\sigma}=\boldsymbol{\nu}\cdot\mathbf{T}$, where $\boldsymbol{\nu}\perp\mathbf{l}$. The expression of the elastic surface stress tensor $\mathbf{T}$ is found basically by noting that $\gamma=\gamma(\mathbf{k})$ and by using the identity $\mathbf{T}=\mathbf{I}_s\cdot\mathbf{T}$. The surface elastic stress tensor $\mathbf{T}$ is given by the usual 2×2 symmetric interfacial tension contribution $\mathbf{T}^n$ (normal stresses) and the 2×3 anisotropic contribution $\mathbf{T}^b$ (bending stresses):

$$\mathbf{T}=\mathbf{T}^n+\mathbf{T}^b,\quad \mathbf{T}^n=\gamma\mathbf{I}_s,\quad \mathbf{T}^b=-\mathbf{I}_s\cdot\left[\frac{\partial\gamma}{\partial\mathbf{k}}\mathbf{k}\right]=-\gamma'\mathbf{n}_\parallel\mathbf{k}. \tag{17}$$

Comparing Eqs. (12), (13), and (17) we find that the correspondence between the surface stress tensor $\mathbf{T}$ and the Cahn-Hoffman capillarity vector $\boldsymbol{\xi}$ is

$$\mathbf{T}=\boldsymbol{\xi}\cdot\boldsymbol{\Psi}, \tag{18a}$$

$$\boldsymbol{\Psi}=\mathbf{k}\mathbf{I}_s-\mathbf{I}_s\mathbf{k}, \tag{18b}$$

$$\mathbf{T}^n=\boldsymbol{\xi}_\perp\mathbf{I}_s,\quad \mathbf{T}^b=-\boldsymbol{\xi}_\parallel\mathbf{k}=\frac{d\gamma}{d\theta}\mathbf{t}_0\mathbf{k}. \tag{18c}$$

The bending coefficient $d\gamma/d\theta$ is the fastest rate of decrease in anchoring energy, and in the principal frame, $\mathbf{T}^b$ has only one component. Figure 5(a) shows the bending stress cylinder, $\mathbf{k}$, $\mathbf{n}$, $\mathbf{t}_0$, $\mathbf{b}_0$, and $|d\gamma/d\theta|$. The arrows denote the direction and magnitude of the bending stresses acting on a surface patch whose orthogonal frame is any arbitrary orthogonal $(\mathbf{t},\mathbf{b})$. The magnitude of the bending stress at any point on the circle is

$$\mathbf{t}\cdot\mathbf{T}^b\cdot\mathbf{k}=\frac{d\gamma}{d\theta}(\mathbf{t}\cdot\mathbf{t}_0)=\frac{d\gamma}{d\theta}\cos\varphi, \tag{19}$$

where φ is the angle between $\mathbf{t}_0$ and $\mathbf{t}$. Figure 5(b) shows that when the frame is $(\mathbf{t}_0,\mathbf{b}_0)$ there is only one component (principal bending stress of magnitude $|d\gamma/d\theta|$) acting on the surface direction normal to $\mathbf{t}_0$. Figure 5(c) shows that for any other $(\mathbf{t},\mathbf{b})$ frame there are two bending stress components, whose magnitudes depend on the rotation angle between the principal frame and the $(\mathbf{t},\mathbf{b})$ frame.

V. APPLICATION OF CAPILLARY VECTOR THERMODYNAMICS: INTERFACE CONFIGURATION AT TRIPLE LINES

The interface configuration at the junction of three flat fluid isotropic interfaces, characterized by interfacial tensions $\{\gamma^{(i)}\}$; $i=1, 2, 3$ is given by the Neumann equation [16]

$$\sum_i \boldsymbol{\sigma}_{\parallel}^{(i)} = \mathbf{0}, \tag{20a}$$

$$\boldsymbol{\sigma}_{\parallel}^{(i)} = \boldsymbol{\xi}_{\perp}^{i} \times \mathbf{l} = \gamma^{(i)}(\mathbf{k}^{(i)} \times \mathbf{l}) = \gamma^{(i)} \boldsymbol{\nu}^{(i)}, \tag{20b}$$

where no line tension energy, long range, and surface anisotropies effects are taken into account, and $\mathbf{l}$ is the unit vector along the straight triple line. In this case all the forces at the triple line are tangential to the three interfaces. Defining the three angles that span each phase as $\varpi^{(i)}$; $i=1, 2, 3$, where $\varpi^{(1)}$ is the dihedral angle limited by interface 2 and 3, gives the interface configuration equation

$$\frac{\gamma^{(1)}}{\sin \varpi^{(1)}} = \frac{\gamma^{(2)}}{\sin \varpi^{(2)}} = \frac{\gamma^{(3)}}{\sin \varpi^{(3)}}. \tag{21}$$

If the three phases are anisotropic, the generalization of the Neumann equation is [14]

$$\sum_i \boldsymbol{\sigma}^{(i)} = \mathbf{0},$$

$$\boldsymbol{\sigma}^{(i)} = \boldsymbol{\xi}^{(i)} \times \mathbf{l} = \boldsymbol{\xi}_{\perp}^{(i)} \times \mathbf{l} + \boldsymbol{\xi}_{\parallel}^{(i)} \times \mathbf{l} = \gamma^{(i)} \boldsymbol{\nu}^{(i)} + \boldsymbol{\xi}_{\parallel}^{(i)} \times \mathbf{l}.$$

Assuming all three flat interfaces have nematic ordering, the configuration at the straight triple line, neglecting any long range contributions, is given by

$$\begin{gathered} \sum_i \boldsymbol{\sigma}^{(i)} = \mathbf{0}, \\ \boldsymbol{\sigma}^{(i)} = \boldsymbol{\xi}^{(i)} \times \mathbf{l} = \gamma^{(i)} \boldsymbol{\nu}^{(i)} + \boldsymbol{\xi}_{\parallel}^{(i)} \times \mathbf{l} = \gamma^{(i)} \boldsymbol{\nu}^{(i)} \\ + \frac{d\gamma^{(i)}}{d(\mathbf{n}^{(i)} \cdot \mathbf{k}^{(i)})} (\mathbf{n}_{\parallel}^{(i)} \times \mathbf{l}). \end{gathered} \tag{22}$$

Introducing the junction sum of capillary vectors $\mathbf{Z}$,

$$\mathbf{Z} = \boldsymbol{\xi}^{(i)} + \boldsymbol{\xi}^{(2)} + \boldsymbol{\xi}^{(3)}, \tag{23}$$

it follows that the nematic configuration obeys

$$\mathbf{Z} \cdot \mathbf{I}_1 = (\boldsymbol{\xi}^{(1)} + \boldsymbol{\xi}^{(2)} + \boldsymbol{\xi}^{(3)}) \cdot \mathbf{I}_1 = \mathbf{0}, \quad \mathbf{I}_1 = \mathbf{I} - \mathbf{ll}, \tag{24}$$

which is the generalization of the Neumann equation for nematic triple lines.

VI. CONCLUSIONS

In summary, the Cahn-Hoffman capillarity vector thermodynamic formalism for anisotropic surfaces has been adapted to nematic liquid crystal surfaces, and its connection with the classical stress tensor model has been established. The Cahn-Hoffman vector formalism offers a clear and tractable methodology to analyze capillarity forces in nematic surfaces. The existence of rotational forces and their connection to gradients of anchoring energy and bending stresses have been established. The potential minimization of anchoring energy leads to surface rotations and bending stresses. The nematic Cahn-Hoffman capillarity vector is an efficient tool to analyze shape selection and surface patterning processes in liquid crystals. The application of the formalism to a straight nematic triple line shows that the interface configuration should be such that the projection of the sum of the three capillarity vectors on a plane normal to the contact line vanishes [16].

ACKNOWLEDGMENT

This work was supported by the Air Force Office of Scientific Research, Mathematical and Space Science Program, under Grant No. F49620-00-1-0341.

[1] A. A. Sonin, *The Surface Physics of Liquid Crystals* (Gordon and Breach, Amsterdam, 1995).
[2] B. Jerome, in *Handbook of Liquid Crystals*, edited by D. Demus, J. Goodby, G. W. Gray, H.-W. Spiess, and V. Vill (Wiley-VCH, Weinheim, 1998), Vol. 1.
[3] H. Yokoyama, in *Handbook of Liquid Crystal Research*, edited by P. J. Collins and J. S. Patel (Oxford University Press, New York, 1997), Chap. 6, p. 179.
[4] T. J. Sluckin and A. Poniewierski, in *Fluid Interfacial Phenomena*, edited by C. A. Croxton (Wiley, Chichester, 1986), Chap. 5.
[5] S. Faetti, in *Physics of Liquid Crystalline Materials*, edited by I.-C. Khoo and F. Simoni (Gordon and Breach, Philadelphia, 1991), Chap. XII, p. 301.
[6] E. G. Virga, *Variational Theories for Liquid Crystals* (Chapman and Hall, London, 1994).
[7] A. K. Sen and D. E. Sullivan, Phys. Rev. A **35**, 1391 (1987).
[8] G. Barbero and G. Durand, in *Liquid Crystals in Complex Geometries*, edited by G. P. Crawford and S. Zumer (Taylor and Francis, London, 1996), p. 21.
[9] J. T. Jenkins and P. J. Barrat, Q. J. Mech. Appl. Math. **27**, 111 (1974).
[10] J. L. Ericksen, in *Advances in Liquid Crystals*, edited by G. H. Brown (Academic, New York, 1979), Vol. 4, p. 1.
[11] C. Papenfuss and W. Muschik, Mol. Mater. **2**, 1 (1992).
[12] A. D. Rey, J. Chem. Phys. **113**, 10 820 (2000).
[13] A. D. Rey, Phys. Rev. E **61**, 1540 (2000).
[14] D. W. Hoffman and J. W. Cahn, Surf. Sci. **31**, 368 (1972).
[15] A. Rapini and M. Papoular, J. Phys. Colloq. **C4**, 54 (1969).
[16] D. A. Edwards, H. Brenner, and D. T. Wasan, *Interfacial Transport Processes and Rheology* (Butterworth-Heinemann, Stoneham, MA, 1991).